

# Methods for Assessing Bone Quality

## A Review

Eve Donnelly PhD

Published online: 30 November 2010  
© The Association of Bone and Joint Surgeons® 2010

### Abstract

**Background** Bone mass, geometry, and tissue material properties contribute to bone structural integrity. Thus, bone strength arises from both bone quantity and quality. Bone quality encompasses the geometric and material factors that contribute to fracture resistance.

**Questions/purposes** This review presents an overview of the methods for assessing bone quality across multiple length scales, their outcomes, and their relative advantages and disadvantages.

**Methods** A PubMed search was conducted to identify methods related to bone mechanical testing, imaging, and compositional analysis. Using various exclusion criteria, articles were selected for inclusion.

**Results** Methods for assessing mechanical properties include whole-bone, bulk tissue, microbeam, and micro- and nanoindentation testing techniques. Outcomes include structural strength and material modulus. Advantages include direct assessment of bone strength; disadvantages include specimen destruction during testing. Methods for characterizing bone geometry and microarchitecture include quantitative CT, high-resolution peripheral quantitative CT, high-resolution MRI, and micro-CT. Outcomes include three-dimensional whole-bone geometry, trabecular morphology, and tissue mineral density. The primary advantage is the ability to image noninvasively; disadvantages include the lack of a direct measure of bone

strength. Methods for measuring tissue composition include scanning electron microscopy, vibrational spectroscopy, nuclear magnetic resonance imaging, and chemical and physical analytical techniques. Outcomes include mineral density and crystallinity, elemental composition, and collagen crosslink composition. Advantages include the detailed material characterization; disadvantages include the need for a biopsy.

**Conclusions** Although no single method can completely characterize bone quality, current noninvasive imaging techniques can be combined with ex vivo mechanical and compositional techniques to provide a comprehensive understanding of bone quality.

### Introduction

Multiple factors contribute to the structural integrity of whole bones: the total bone mass, the bone geometry, and the properties of the constituent tissue [80]. Despite the multiplicity of contributors to bone strength, one factor is primarily used clinically to diagnose osteoporosis and assess fracture risk: bone mass, characterized by bone mineral density (BMD) assessed by dual-energy x-ray absorptiometry [24]. Because BMD is a limited predictor of fracture risk [58], clinical and scientific interest has increased in complementary measures of bone quality that could improve fracture risk prediction [10].

Throughout this review, the working definition of bone quality encompasses all of the geometric and material factors contributing to fracture resistance. Geometric factors include the macroscopic geometry of the whole bone and the microscopic architecture of the trabeculae. Material factors include the material properties of the constituent tissue arising from the composition and arrangement of the

The author has received funding from the National Institutes of Health (F32 AR056148-02).

E. Donnelly (✉)  
Mineralized Tissues Laboratory, Hospital for Special Surgery,  
535 East 70th Street, New York, NY 10021, USA  
e-mail: donnellye@hss.edu

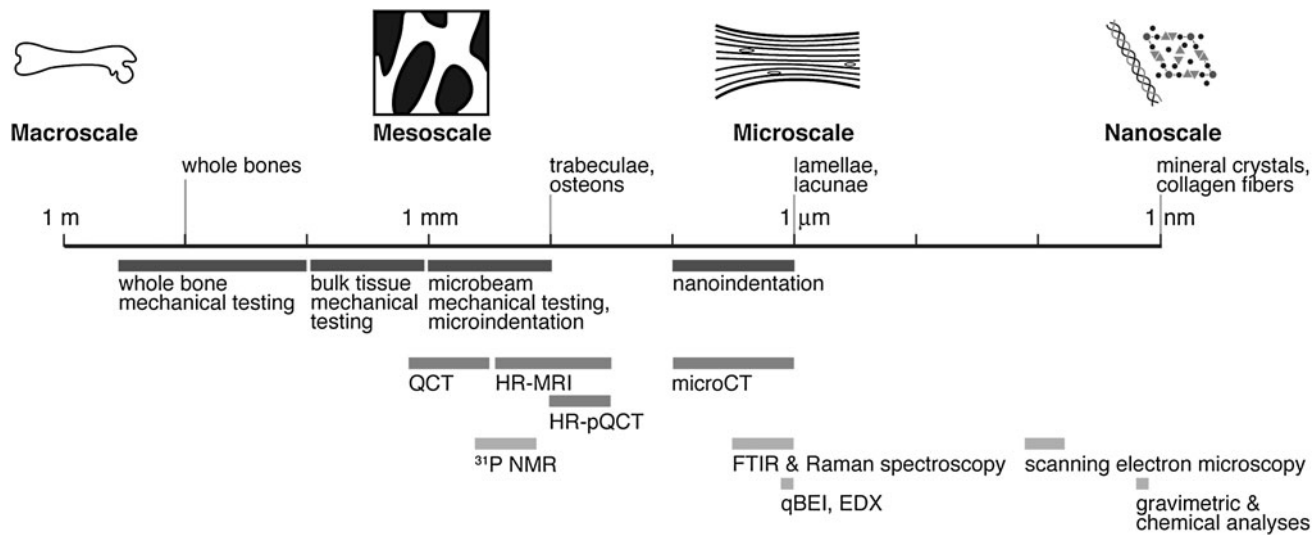


**Fig. 1** The hierarchical structure of bone is depicted schematically on a logarithmic scale. Techniques for mechanical (dark gray bars), geometric/microarchitectural (medium gray bars), and compositional

(light gray bars) are shown according to their approximate length scale of analysis.

primary microstructural constituents, collagen and mineral, as well as microdamage and microstructural discontinuities such as microporosity and lamellar boundaries. Inclusion of microarchitectural and material measures in addition to BMD improves prediction of bone strength and fracture risk relative to that from BMD alone [34, 35].

This review presents an overview of the techniques available to assess bone mechanical properties, geometry and microarchitecture, and composition across multiple hierarchical levels (Fig. 1). Relatively new techniques are emphasized because existing reviews cover established histomorphometric, radiographic, densitometric, and clinical imaging techniques [4, 24, 53, 65]. Many of the techniques addressed here are presented individually in this symposium, and this review should serve as a comparative reference; readers are referred to other symposium articles for more details on each method.

The following key questions are addressed: (1) What are the techniques currently available for assessment of the mechanical, geometric, and material components of bone quality? (2) What are the main outcomes of each method? (3) What are the relative advantages and limitations of these methods?

## Search Strategy and Criteria

A PubMed search of all published literature in the English language from January 1966 to December 2009 was performed for the following sets of key words: (1) “bone AND mechanical testing methods AND (cancellous OR cortical) NOT (screw OR plate OR implant OR prosthesis),” which

yielded 155 articles, four of which were review articles; (2) “bone AND microindentation,” which yielded 14 articles, zero of which were review articles; (3) “bone AND nano-indentation,” which yielded 153 articles, four of which were review articles; (4) “bone AND quantitative computed tomography AND (methodologies OR methods) AND resolution,” which yielded 200 articles, 26 of which were review articles; (5) “bone AND high resolution peripheral quantitative computed tomography AND (methodologies OR methods),” which yielded 49 articles, five of which were review articles; (6) “bone AND high resolution magnetic resonance imaging AND methods NOT (cartilage OR angiography OR tumor),” which yielded 461 articles, 66 of which were review articles; (7) “bone AND high resolution micro computed tomography,” which yielded 170 articles, 16 of which were review articles; (8) “bone AND NMR imaging AND (31P OR solid state OR bound water),” which yielded 57 articles, eight of which were review articles; (9) “bone AND FTIR imaging,” which yielded 74 articles, five of which were review articles; (10) “bone AND Raman imaging,” which yielded 30 articles, five of which were review articles; (11) “bone AND (scanning electron microscopy OR backscattered electron OR energy dispersive x-ray) AND (methodologies OR methods) NOT (allograft OR bone substitute OR implant OR scaffold OR cartilage),” which yielded 1321 articles, 34 of which were review articles; (12) “bone AND gravimetric analysis NOT (disc OR composites OR polyethylene OR scaffold OR prosthesis),” which yielded 31 articles, zero of which were review articles; and (13) “bone AND collagen AND cross-links AND (HPLC OR fluorescence),” which yielded 63 articles, one of which was a review article.

After a review of the titles, articles were excluded if they pertained primarily to cells in culture, tissue-engineered constructs, bone cement, bone-implant interfaces, mineralized tissues other than bone, synthetic biomaterials, or geologic minerals. Articles on imaging modalities were also excluded if their primary focus was on vasculature, tumors, or soft tissues such as cartilage, tendon, or meniscus. For the imaging modalities for which the searches yielded more than 100 articles, articles focusing on methodology were prioritized. Then the review articles were examined, and relevant references from those articles were identified in the specific areas of interest. This yielded approximately 150 articles.

### Assessment of Bone Mechanical Properties

Mechanical testing allows direct assessment of a range of mechanical properties across multiple length scales (Fig. 1), allowing characterization of multiple structural and material properties (Table 1). At the macroscopic level, whole-bone testing allows assessment of bone structural properties such as structural stiffness and strength. At smaller length scales, material testing techniques enable measurement of the intrinsic properties of the tissue such as elastic modulus and ultimate stress.

#### Whole-bone Mechanical Testing

At the macroscale, the structural behavior of bones is assessed by whole-bone mechanical testing. In these tests, a whole bone is typically loaded to failure in compression, bending, or torsion [79, 80]. Outcomes include the structural stiffness, the failure load, and the energy absorbed to failure. The structural stiffness represents the bone's resistance to elastic, or reversible, deformation. The failure load characterizes the strength of the bone. The energy absorbed to failure is a measure of structural toughness and represents the energy the bone can absorb before it breaks. Experimental assessment of bone strength requires destructive whole-bone testing, and an inherent limitation of testing to failure is that the specimen is broken during testing.

#### Bulk Tissue Specimen Testing

Mechanical testing of bulk tissue specimens excised from whole bones is used to assess the mechanical properties of cortical and cancellous tissue. This type of testing has been used to characterize the effects of a wide range of variables, including anatomic site [33, 60], porosity [27],

apparent density [19], and tissue mineral content [15, 26], on the mechanical properties of bone tissue. In these tests, regularly shaped specimens (typically cylinders or cubes with diameters or edge lengths of 5–10 mm) are machined from cortical or cancellous tissue and tested to failure in tension, compression, bending, or torsion [46, 68]. Outcomes include the effective elastic modulus and ultimate stress. The effective material properties obtained from these tests are independent of the macroscopic bone geometry but include the effects of porosity and geometric anisotropy arising from osteon or trabecular orientation.

#### Microbeam Testing

Techniques using microbeam specimens have been developed to isolate the material properties of bone tissue [20, 47]. In these tests, bending or tensile loads are applied to microbeams (approximately  $200 \times 200 \times 2000 \mu\text{m}$ ) machined from trabecular and cortical bone [20, 47, 78]. Outcomes include the elastic modulus and ultimate stress. The elastic modulus characterizes the material's intrinsic resistance to elastic (reversible) deformation. The yield stress characterizes the material's intrinsic resistance to plastic (permanent) deformation. The material properties obtained from these tests are independent of the macroscopic bone geometry and trabecular microarchitecture yet still include the effects of discontinuities such as lamellar boundaries and microscale porosity due to lacunae and resorption sites [37].

#### Microindentation

Alternatively, classical indentation testing can be used to test the material properties of bone tissue at the meso- to microscale. In an indentation test, a rigid indenter is pressed with a known force into a flat specimen, and the area of the resulting impression is estimated optically [89]. The hardness is defined as the force divided by the area of the imprint and characterizes the material's resistance to plastic deformation. Microindentation allows characterization of the mechanical properties of individual trabeculae or osteons [88, 89]. Advantages include the relative ease of testing and the ability to make measurements in multiple locations within the tissue. A drawback of this technique is that its sole outcome is the tissue hardness.

Although few techniques are currently available for *in vivo* characterization of bone mechanical properties, an *in vivo* system capable of applying loads through an indenter within a hypodermic needle is under development [36]. This technique is currently limited to superficial sites

**Table 1.** Summary of methods of assessment of bone quality with key outcomes, in vivo/ex vivo measurement capability, and length scale

Category	Method	Mechanical outcomes	Geometric/microstructural outcomes	Compositional outcomes	Ex vivo or in vivo?	Spatially resolved?	Specimen preparation
Mechanical methods	Whole-bone mechanical testing	Structural strength, stiffness			Ex vivo	No	
	Bulk tissue specimen mechanical testing	Effective modulus, ultimate stress			Ex vivo	No	Specimen machining
	Microbeam mechanical testing	Material modulus, ultimate stress			Ex vivo	No	Specimen machining
	Microindentation	Material hardness			Ex vivo; in vivo in development	Yes	Surface polishing
Imaging methods	Nanoindentation	Material indentation modulus, hardness			Ex vivo	Yes	Surface polishing
	QCT	3D bone geometry, apparent BMD			In vivo	Yes	
	HR-pMRI	3D bone geometry, trabecular morphology			In vivo	Yes	
	HR-pQCT	3D bone geometry, trabecular morphology, apparent BMD			In vivo	Yes	
Micro-CT	Micro-CT	3D bone geometry: BV/TV; trabecular thickness, separation, number, connectivity	Tissue mineral density		Ex vivo; in vivo for small rodents	Yes	
	NMR imaging	3D distribution of bone water or mineral	Volume % bone water, BMD	Ex vivo, in vivo	Yes		
	FTIR imaging		Mineral:matrix, carbonate/phosphate, collagen maturity, crystal size/perfection	In vitro	Yes	Dehydration, embedding, sectioning	
	Raman imaging		Mineral:matrix, carbonate: phosphate, crystallinity	Ex vivo; in vivo for rodents	Yes	Surface polishing	
Chemical/physical methods	Scanning electron microscopy/qBEI/EDX	Dimensions of microstructural features	Elemental composition (calcium/phosphorus), tissue density	In vitro	Yes	Dehydration, surface polishing, conductive coating	
	Gravimetric analysis (ashing)		Ash%	In vitro	No		
	Chemical analysis of collagen crosslinks	Total collagen	Total collagen	In vitro	No	Radiolabeling, hydrolysis	

QCT = quantitative CT; HR-MRI = high-resolution peripheral quantitative CT; NMR = nuclear magnetic resonance imaging; FTIR = Fourier transform infrared; qBEI = quantitative backscattered electron imaging; EDX = energy-dispersive x-ray analysis; 3D = three-dimensional; BMD = bone mineral density; BV/TV = bone volume fraction.

such as the tibial midshaft, and its outcomes remain to be validated. Nevertheless, it represents a first step toward in vivo characterization of tissue material properties.

### Nanoindentation

At the microscale, nanoindentation is capable of probing the mechanical properties of volumes of tissue as small as individual lamellae. In this technique, an indentation test is performed with a depth-sensing indenter tip, often combined with a scanning probe microscope for spatially resolved measurements. The force-displacement data are analyzed to obtain the indentation modulus and hardness [64]. Nanoindentation with relatively shallow indentation depths of approximately 100 nm yields spatial resolutions of approximately 1  $\mu\text{m}$  in bone tissue [38]. Advantages of this technique include the capability to measure the material properties of microstructural features such as lamellae [29, 38, 69] and to detect localized changes in bone material properties induced by disease or drug treatment [50]. Disadvantages include the need for relatively specialized instrumentation and very smooth specimens if the highest level of spatial resolution is required [28].

## Assessment of Bone Geometry and Microarchitecture

A variety of imaging techniques allow characterization of bone geometry and microarchitecture from the macroscale to the nanoscale (Fig. 1). Most imaging techniques allow for multiple measurements within the same individual over time, making them well suited to longitudinal studies.

### Quantitative CT

Macroscopic assessment of three-dimensional (3D) bone geometry can be performed in vivo using quantitative CT (QCT) [32]. In QCT, an x-ray source produces x-rays that are attenuated by an object of interest, and a detector on the opposite side detects the signal. The source and detector rotate about the object, and tomographic algorithms are used to construct a 3D image of x-ray attenuation. QCT outcomes include the 3D macroscopic bone geometry in which the cortical and trabecular bone are distinct and apparent volumetric BMD (vBMD, mass mineral/total volume [bone + marrow]). The ability to image vertebral sites is a strength of this method, although its in-plane resolution (approximately 0.5 mm) is insufficient to resolve trabecular architecture [32]. An important drawback of QCT is its delivery of ionizing radiation to patients.

### High-resolution Peripheral QCT

The advent of high-resolution peripheral QCT (HR-pQCT) scanners with isotropic resolution of approximately 80  $\mu\text{m}$  has enabled in vivo imaging of 3D trabecular morphology at peripheral sites such as the distal radius [9, 43]. The primary advantage of this technique is that trabecular bone can be resolved, and morphologic parameters such as bone volume fraction (BV/TV), trabecular thickness (Tb.Th), trabecular separation (Tb.Sp), and trabecular number (Tb.N) can be calculated. Inclusion of calibration phantoms also allows calculation of apparent vBMD. Because the spatial resolution approaches the size of trabeculae, partial volume effects affect the morphologic parameters; nevertheless, the HR-pQCT trabecular measures are correlated with those assessed by micro-CT, the current gold standard for quantification of trabecular morphology [55]. These measurements are largely restricted to peripheral sites but have the concomitant benefit of reduced radiation doses relative to those from whole-body QCT scans.

### High-resolution MRI

High-resolution MRI (HR-MRI) allows nonionizing 3D imaging of the trabecular network at peripheral sites. During scanning, a strong magnetic field and a series of radiofrequency (RF) pulses are applied to the specimen to generate 3D images of the hydrogen in the water within skeletal tissues. Bone tissue generates no signal in standard MR images as a result of the low water content of the tissue and the chemical environment of the protons within the bone matrix. Rather, when the marrow is imaged, the trabeculae appear as the dark space within the bright marrow [17]. Resolutions as small as approximately 50  $\times$  50  $\times$  200  $\mu\text{m}$  have been achieved ex vivo [21], and resolutions of 156  $\times$  156  $\times$  300  $\mu\text{m}$  are typical in vivo [43]. Consequently, MRI-based trabecular morphologic parameters are also affected by partial volume effects [57]. The MRI-based trabecular measures are correlated with their counterparts measured by micro-CT, and MRI can detect age- and disease-induced changes in trabecular morphology [56]. A critical advantage of this technique is its ability to generate 3D images of bone geometry and microarchitecture without ionizing radiation; disadvantages include the long scan times required for high-resolution images of trabecular bone.

### Micro-CT

At the microscale, micro-CT provides ex vivo characterization of trabecular microarchitecture with isotropic resolutions as small as 1 to 6  $\mu\text{m}$ . In micro-CT scanners,

the specimen is rotated in angular increments between the x-ray source and detector, and the attenuation data at each position are reconstructed into a 3D array of x-ray attenuation, which can be converted to mineral density values with inclusion of appropriate calibration phantoms [73]. Outcomes include BV/TV, Tb.Th, Tb.Sp, Tb.N, trabecular connectivity, and true tissue mineral density (TMD, mass mineral/volume bone tissue). Limitations include a maximum specimen size of approximately 14-mm diameter  $\times$  36-mm length in older scanners and 100-mm diameter  $\times$  140-mm length in newer scanners [73]. Nevertheless, micro-CT has become the workhorse technique for ex vivo quantification of trabecular morphology.

The development of desktop in vivo micro-CT scanners has enabled characterization of the macroscopic geometry and microarchitecture of the bones of living animals. Such scanners have enabled longitudinal studies examining skeletal development, adaptation, and response to treatment within the same animals at an isotropic resolution up to approximately 10  $\mu\text{m}$ , although high resolutions require relatively long scan times and large radiation doses [41, 83]. Limitations of these studies include their restriction to small rodents and the need to moderate the ionizing radiation received by the study animals.

At the highest resolution, micro-CT in vivo or ex vivo with a synchrotron source maximizes resolution of micro-architectural features and local spatial gradients in tissue mineral content. The tightly collimated, monochromatic x-ray source provides an isotropic spatial resolution of approximately 1  $\mu\text{m}$  and eliminates the beam hardening artifacts arising from differential attenuation of the polychromatic sources in conventional desktop micro-CT systems [42, 66]. Synchrotron micro-CT is the current gold standard for assessment of local gradients in TMD [42] and is capable of resolving resorption spaces [66] and microcracks [82]. However, the relative inaccessibility of synchrotron facilities limits the widespread use of this technique.

### Assessment of Tissue Composition

Both the inorganic and the organic components of bone tissue contribute to the structural integrity of whole bones [3, 15, 25, 81]. Microscopic, spectroscopic, physical, and chemical techniques are available for characterization of the mineral and the collagenous components of bone tissue.

#### Nuclear Magnetic Resonance Imaging

Nuclear magnetic resonance (NMR) imaging provides information about water content and the structure of the mineral within the tissue. For analyses of water and mineral

in bone, the primary isotopes of interest are  $^1\text{H}$  and  $^{31}\text{P}$ , respectively. As in MRI, when placed in a strong magnetic field, the NMR-active  $^1\text{H}$  and  $^{31}\text{P}$  nuclei in the bone mineral resonate at slightly different frequencies depending on their local chemical environment, and NMR spectra are generated by varying the frequency of the applied RF field and monitoring the absorption of the specimen [84].

Water in bone tissue, while not detected with typical clinical MRI techniques, can be imaged with appropriate pulse sequences [77]. The volume percent of bone water (%BW) can be quantified from the  $^1\text{H}$  images and can serve as a surrogate measure of cortical porosity. The %BW is inversely correlated with effective ultimate stress estimated from three-point bending tests of cadaveric bones [31, 63].

Solid-state  $^{31}\text{P}$  NMR imaging can be used to characterize the chemical structure of bone mineral, allowing detection of temporal changes in the mineral chemistry [48]. Furthermore, this technique can be used quantitatively to determine the mass of bone mineral in the tissue [85], enabling detection of hypomineralization in osteomalacic rabbit tissue at an isotropic spatial resolution of approximately 280  $\mu\text{m}$  [1]. Quantitative NMR analyses of bone mineral chemistry have also been performed in vivo, but such studies typically require long acquisition times in specialized scanners and are currently limited to the fingers, wrist, and hand [13, 22, 86]. Recent advances in instrumentation have enabled in vivo solid state imaging of bone mineral in a clinical scanner [87].

NMR techniques allow noninvasive, nonionizing in vivo characterization of changes in the composition of bone tissue. Strengths of NMR include the ability to detect subtle changes in the chemical bonding environments of the bone mineral, but this technique cannot provide information about the collagenous component of the matrix. The low signal-to-noise ratio and limited spatial resolution remain key challenges for the  $^{31}\text{P}$  solid state methods [59].

#### Vibrational Spectroscopic Imaging: Fourier Transform Infrared and Raman Imaging

Vibrational spectroscopy, including Fourier transform infrared (FTIR) and Raman techniques, characterizes the chemical composition and bonding environments of the tissue constituents. In these techniques, incident light focused on the specimen excites vibrations of the chemical bonds in the mineral and protein components of the tissue. These vibrations are excited at characteristic frequencies corresponding to absorption peaks on an infrared (IR) or Raman spectrum and can be analyzed to characterize tissue composition [7, 18]. More recently, the coupling of an IR or Raman spectrometer with an optical microscope and a

focal plane array detector has greatly enhanced the utility of these techniques by enabling spatial mapping of microscale tissue composition [7]. Both FTIR imaging and Raman imaging can be used to examine changes in tissue properties with developmental stage, tissue age, or disease within a bone specimen.

Outcomes of FTIR spectroscopy include measures of the relative mineral and matrix content (mineral:matrix ratio), carbonate substitution into the mineral lattice (carbonate:phosphate ratio) collagen crosslink maturity (collagen crosslink ratio), and mineral crystal size and perfection (crystallinity); and incorporation of FTIR properties into statistical models improves the prediction of fracture risk over models with BMD alone [8]. The spatial distribution of each of these properties can be characterized at a spatial resolution of approximately 6 μm [7]. Because FTIR imaging is conducted in transmission, relatively thin (approximately 2-μm), dehydrated sections of undecalcified bone are required. Strengths of this method include the relatively established nature of the technique and multiple validated outcomes that have been related to fracture risk; limitations include the requirement for dehydrated, thin sections of bone.

Similar to the outcomes of FTIR spectroscopy, Raman spectroscopy has analogous measures of the mineral:matrix ratio, carbonate:phosphate ratio, and mineral crystallinity; and Raman imaging can be used to generate compositional maps with spatial resolution of approximately 1 μm [18]. Imaging can be performed in reflectance on thick, hydrated specimens [18]. Although the use of Raman spectroscopy to study bone tissue is somewhat less established than the use of FTIR, its superior spatial resolution and ability to image hydrated specimens make it advantageous for examining fine gradients in tissue composition and for use in tissues under physiologic conditions.

Indeed, although most Raman spectroscopy is conducted ex vivo, in vivo probes capable of collecting Raman spectra transcutaneously have been developed recently. Initial systems were able to distinguish mineralization defects in tissue from mice with osteogenesis imperfecta versus that from wild-type controls [30], and subsequent improvements have resulted in improved signal intensity and power distributions [74]. This technique is currently limited to superficial sites with minimal overlying soft tissue, and applications to date are limited to preclinical studies. Nevertheless, this method remains a promising step toward noninvasive diagnostic assessment of bone tissue composition.

### Scanning Electron Microscopy

Scanning electron microscopy allows characterization of the morphology and composition of bone surfaces. In this

technique, an electron beam is focused and scanned across the specimen surface, and the electrons interact with the atoms in the sample and generate three types of signals: secondary electrons (SEs), backscattered electrons (BSEs), and xrays. In secondary electron imaging (SEI), SEs are generated when an incident electron imparts some of its energy to an atom in the specimen, causing emission of a low-energy ionized electron from the specimen. The SE signal arises from the specimen surface and provides excellent topographic detail at a resolution of approximately 20 nm [11]. In quantitative backscattered electron imaging (qBEI), BSEs are generated when an incident electron collides with an atom in the specimen and is scattered “backward.” Because the intensity of the BSE signal is proportional to the atomic number of the specimen, the gray-level intensity values in a BSE image can be related to TMD [5], and maps of TMD can be collected at a spatial resolution of approximately 1 μm [72]. Energy-dispersive xray (EDX) microanalysis involves analysis of xrays with energies characteristic of the atoms in the specimen emitted when an incident electron hits the specimen surface [40]. Analysis of these xrays can provide elemental maps of the distribution of important elements such as Ca, P, F, and Sr within the specimen [49, 71].

The excitation volumes for BSEs and xrays are larger than those for SEs, resulting in reduced spatial resolution for qBEI and EDX images relative to SEI images [39, 40]. However, qBEI and EDX analyses provide important quantitative compositional information that can be used in conjunction with SEI images to relate composition to lamellar topography, resorption spaces, and microcracks. Limitations of scanning electron microscopy-based quantitative techniques include the need to dehydrate and coat the specimen with a conductive coating.

### Gravimetric Analyses

Gravimetric analysis provides a straightforward method for determination of the mineral content of bone tissue. Typically, bones are dried at 110°C, weighed to determine the dry weight of the tissue, and then heated to 600°C to remove the organic matrix [6]. The weight of the remaining mineral phase, the ash weight, can be normalized to the dry weight of the tissue to give the ash fraction. If the volume of the bone is known or measured by water displacement, then the ash density can be determined by dividing the ash weight by the bone volume. A major advantage of this technique is its relative simplicity, but it requires homogenization of the tissue and cannot characterize the spatial distribution of the mineral within the bone.

## Chemical Analysis of Collagen Crosslinks

Collagen in bone tissue specimens can be analyzed quantitatively to determine the total quantity of collagen and the types of crosslinks present. The total amount of collagen and the extent of nonenzymatic glycation can be analyzed relatively straightforwardly using fluorescence measurements [75, 76]. More detailed analyses of collagen crosslink chemistry require high-pressure liquid chromatography (HPLC) techniques. Tissue specimens can be hydrolyzed and analyzed with HPLC to determine relative quantities of immature (hydroxylysionorleucine and dihydroxylysionoroleucine) and mature (hydroxylysylpyridinoline and lysyl-pyridinoline) crosslinks [2]. These chemical methods are able to detect subtle differences in the chemistry of the organic matrix constituents, but they require homogenization of the tissue, and the HPLC methods require specialized expertise and equipment.

## Discussion

This review summarized the techniques available to assess bone quality (Fig. 1), their outcomes (Table 1), and their advantages and disadvantages. The techniques described here provide complementary data on mechanical properties, geometry/microarchitecture, and material properties. Characterization of bone geometry and material properties can be used in conjunction with mechanical testing to identify the relative contributions of geometry and material properties to bone structural integrity. While all of the techniques described here have disadvantages, their shortcomings can be mitigated by employing multiple techniques with complementary outcomes.

This review has several limitations. First, relatively new techniques were emphasized over more established histomorphometric, radiographic, densitometric, and clinical imaging methods; however, existing articles [4, 24, 53, 65] provide comprehensive reviews of these methods. Second, this review addressed only experimental methods for assessment of bone quality and did not cover computational methods such as finite element analysis, which are reviewed elsewhere [44, 62]. Finally, the broad scope of the review allowed for only a brief summary of each technique. Most of the techniques addressed in this overview are presented in greater depth in this symposium, and readers are referred to these articles for more details on each method. Limitations of the existing literature include the widely varying depth and breadth of available information on each technique, from the tens of thousands of studies available on mature technologies such as CT to the much more limited number of studies examining recent innovations such as in vivo Raman spectroscopy [30, 74]

and in vivo indentation testing [36]. The emerging technologies discussed here require further validation before their widespread adoption in the clinic.

The methods available for assessment of bone quality include techniques for characterization of bone mechanical properties, geometry/microarchitecture, and composition. Selection of experimental methods depends on the study design and the outcomes of interest. Investigations involving an animal model or cadaveric specimens allow for direct assessment of bone strength with destructive mechanical testing [12, 33, 60, 61]. Studies examining bone healing, adaptation to disuse or loading, or response to treatment benefit from imaging methods capable of capturing longitudinal changes in bone geometry or microarchitecture [14, 51, 52, 54, 61]. Studies of patients with altered mechanical properties, eg, in osteogenesis imperfecta [16, 70], require compositional analyses capable of capturing changes in tissue mineral and matrix properties. The methods used to assess bone quality must therefore be tailored to the study design and the outcomes of interest.

The advantages and disadvantages of each technique also relate to study design and the outcomes of interest; in particular, many clinical studies require noninvasive techniques, yet the current noninvasive methods available to clinicians typically provide incomplete information about bone quality. While most of the methods described here are not used in routine clinical practice, many have (or have the potential) to transition from ex vivo research techniques to in vivo research techniques and eventually to clinical methods. The CT- and MRI-based techniques, for example, allow noninvasive assessment of bone geometry at all but the smallest length scales, allowing for multiple measurements within the same individual over time [43]. Micro-CT and NMR imaging allow for simultaneous assessment of tissue composition and bone geometry, enabling spatially and temporally resolved measurements of tissue geometry and mineral composition [73, 87]. In contrast, most of the mechanical and compositional characterization methods require a biopsy but provide a wealth of mechanical and compositional information otherwise unavailable noninvasively [3, 7, 11, 79, 89]. Destructive mechanical testing is necessary for direct assessment of bone strength and remains essential to characterization of bone structural performance. In cases for which destructive testing is not possible, computational techniques, such as finite element analysis based on QCT, HR-pQCT, or micro-CT images, offer a nondestructive alternative for prediction of bone structural properties [23, 45, 67]. Finally, compositional measurements using spectroscopic or chemical techniques provide detailed information about mineral and matrix composition [3, 7, 18, 48] that may yield mechanistic insights into factors affecting bone quality.

None of the noninvasive methods can currently provide a complete assessment of bone quality, but noninvasive imaging techniques can be combined with compositional and mechanical techniques requiring a biopsy to provide a comprehensive understanding of bone quality. Furthermore, although some of the microscale methods discussed in this article are not likely to become noninvasive diagnostic techniques due to inherent experimental limitations, others methods offer promise for characterization of bone quality in the clinic.

**Acknowledgments** I thank Dr. Adele Boskey and Dr. Marjolein van der Meulen for critical review of this manuscript.

## References

- Anumula S, Magland J, Wehrli SL, Zhang H, Ong H, Song HK, Wehrli FW. Measurement of phosphorus content in normal and osteomalacic rabbit bone by solid-state 3D radial imaging. *Magn Reson Med.* 2006;56:946–952.
- Avery NC, Sims TJ, Bailey AJ. Quantitative determination of collagen cross-links. *Methods Mol Biol.* 2009;522:103–121.
- Bailey AJ, Sims TJ, Ebbesen EN, Mansell JP, Thomsen JS, Mosekilde L. Age-related changes in the biochemical properties of human cancellous bone collagen: relationship to bone strength. *Calcif Tissue Int.* 1999;65:203–210.
- Bauer JS, Link TM. Advances in osteoporosis imaging. *Eur J Radiol.* 2009;71:440–449.
- Bloebaum RD, Skedros JG, Vajda EG, Bachus KN, Constantz BR. Determining mineral content variations in bone using backscattered electron imaging. *Bone.* 1997;20:485–490.
- Boskey A. Bone mineralization. In: Cowin SC, ed. *Bone Mechanics Handbook.* 2nd ed. Boca Raton, FL: CRC Press; 2001: 5.1–5.33.
- Boskey A, Mendelsohn R. Infrared analysis of bone in health and disease. *J Biomed Opt.* 2005;10:031102.
- Boskey A, Pleshko Camacho N. FT-IR imaging of native and tissue-engineered bone and cartilage. *Biomaterials.* 2007;28: 2465–2478.
- Boutroy S, Bouxsein ML, Munoz F, Delmas PD. In vivo assessment of trabecular bone microarchitecture by high-resolution peripheral quantitative computed tomography. *J Clin Endocrinol Metab.* 2005;90:6508–6515.
- Bouxsein ML. Bone quality: where do we go from here? *Osteoporos Int.* 2003;14(Suppl 5):S118–S127.
- Boyde A. Scanning electron microscope studies of bone. In: Bourne GH, ed. *The Biochemistry and Physiology of Bone.* 2nd ed. New York, NY: Academic Press; 1972:259–310.
- Brodt MD, Ellis CB, Silva MJ. Growing C57Bl/6 mice increase whole bone mechanical properties by increasing geometric and material properties. *J Bone Miner Res.* 1999;14:2159–2166.
- Brown CE, Battocletti JH, Srinivasan R, Allaway JR, Moore J, Sigmann P. In vivo 31P nuclear magnetic resonance spectroscopy of bone mineral for evaluation of osteoporosis. *Clin Chem.* 1988; 34:1431–1438.
- Burghardt AJ, Kazakia GJ, Sode M, de Papp AE, Link TM, Majumdar S. A longitudinal HR-pQCT study of alendronate treatment in post-menopausal women with low bone density: relations between density, cortical and trabecular microarchitecture, biomechanics, and bone turnover. *J Bone Miner Res.* 2010 June 18 [Epub ahead of print].
- Camacho NP, Hou L, Toledano TR, Ilg WA, Brayton CF, Raggio CL, Root L, Boskey AL. The material basis for reduced mechanical properties in oim mice bones. *J Bone Miner Res.* 1999;14:264–272.
- Carballido-Gamio J, Majumdar S. Clinical utility of microarchitecture measurements of trabecular bone. *Curr Osteoporos Rep.* 2006;4:64–70.
- Carden A, Morris MD. Application of vibrational spectroscopy to the study of mineralized tissues (review). *J Biomed Opt.* 2000;5: 259–268.
- Carter DR, Hayes WC. The compressive behavior of bone as a two-phase porous structure. *J Bone Joint Surg Am.* 1977;59: 954–962.
- Choi K, Kuhn JL, Ciarelli MJ, Goldstein SA. The elastic moduli of human subchondral, trabecular, and cortical bone tissue and the size-dependency of cortical bone modulus. *J Biomech.* 1990; 23:1103–1113.
- Chung HW, Wehrli FW, Williams JL, Kugelmass SD, Wehrli SL. Quantitative analysis of trabecular microstructure by 400 MHz nuclear magnetic resonance imaging. *J Bone Miner Res.* 1995;10: 803–811.
- Code RF, Harrison JE, McNeill KG. In vivo measurement of accumulated bone fluorides by nuclear magnetic resonance. *J Bone Miner Res.* 1990;5(Suppl 1):S91–S94.
- Crawford RP, Cann CE, Keaveny TM. Finite element models predict in vitro vertebral body compressive strength better than quantitative computed tomography. *Bone.* 2003;33:744–750.
- Cummings SR, Bates D, Black DM. Clinical use of bone densitometry: scientific review. *JAMA.* 2002;288:1889–1897.
- Currey JD. The mechanical consequences of variation in the mineral content of bone. *J Biomech.* 1969;2:1–11.
- Currey JD. The relationship between the stiffness and the mineral content of bone. *J Biomech.* 1969;2:477–480.
- Currey JD. The effect of porosity and mineral content on the Young's modulus of elasticity of compact bone. *J Biomech.* 1988;21:131–139.
- Donnelly E, Baker SP, Boskey AL, van der Meulen MC. Effects of surface roughness and maximum load on the mechanical properties of cancellous bone measured by nanoindentation. *J Biomed Mater Res A.* 2006;77:426–435.
- Donnelly E, Williams RM, Downs SA, Dickinson ME, Baker SP, van der Meulen MC. Quasistatic and dynamic nanomechanical properties of cancellous bone tissue relate to collagen content and organization. *J Mater Res.* 2006;21:2106–2117.
- Draper ER, Morris MD, Camacho NP, Matousek P, Towrie M, Parker AW, Goodship AE. Novel assessment of bone using time-resolved transcutaneous Raman spectroscopy. *J Bone Miner Res.* 2005;20:1968–1972.
- Fernandez-Seara MA, Wehrli SL, Takahashi M, Wehrli FW. Water content measured by proton-deuteron exchange NMR predicts bone mineral density and mechanical properties. *J Bone Miner Res.* 2004;19:289–296.
- Genant HK, Engelke K, Prevrhal S. Advanced CT bone imaging in osteoporosis. *Rheumatology (Oxford).* 2008;47(Suppl 4): iv9–iv16.
- Goldstein SA, Wilson DL, Sonstegard DA, Matthews LS. The mechanical properties of human tibial trabecular bone as a function of metaphyseal location. *J Biomech.* 1983;16:965–969.
- Gordon CL, Lang TF, Augat P, Genant HK. Image-based assessment of spinal trabecular bone structure from high-resolution CT images. *Osteoporos Int.* 1998;8:317–325.
- Gourion-Arsiquaud S, Faibis D, Myers E, Spevak L, Compston J, Hodson A, Shane E, Recker RR, Boskey ER, Boskey AL.

- Use of FTIR spectroscopic imaging to identify parameters associated with fragility fracture. *J Bone Miner Res.* 2009;24:1565–1571.
36. Hansma P, Turner P, Drake B, Yurtsev E, Proctor A, Mathews P, Lulejian J, Randall C, Adams J, Jungmann R, Garza-de-Leon F, Fanter G, Mkrtchyan H, Pontin M, Weaver A, Brown MB, Sahar N, Rossello R, Kohn D. The bone diagnostic instrument II: indentation distance increase. *Rev Sci Instrum.* 2008;79:064303.
  37. Hengsberger S, Enstroem J, Peyrin F, Zysset P. How is the indentation modulus of bone tissue related to its macroscopic elastic response? A validation study. *J Biomech.* 2003;36:1503–1509.
  38. Hengsberger S, Kulik A, Zysset P. Nanoindentation discriminates the elastic properties of individual human bone lamellae under dry and physiological conditions. *Bone.* 2002;30:178–184.
  39. Howell PG, Boyde A. Monte Carlo simulations of electron scattering in bone. *Bone.* 1994;15:285–291.
  40. Howell PG, Boyde A. Volumes from which calcium and phosphorus X-rays arise in electron probe emission microanalysis of bone: Monte Carlo simulation. *Calcif Tissue Int.* 2003;72:745–749.
  41. Judex S, Boyd S, Qin YX, Miller L, Muller R, Rubin C. Combining high-resolution micro-computed tomography with material composition to define the quality of bone tissue. *Curr Osteoporos Rep.* 2003;1:11–19.
  42. Kazakia GJ, Burghardt AJ, Cheung S, Majumdar S. Assessment of bone tissue mineralization by conventional x-ray microcomputed tomography: comparison with synchrotron radiation microcomputed tomography and ash measurements. *Med Phys.* 2008;35:3170–3179.
  43. Kazakia GJ, Majumdar S. New imaging technologies in the diagnosis of osteoporosis. *Rev Endocr Metab Disord.* 2006;7:67–74.
  44. Keaveny TM. Biomechanical computed tomography-noninvasive bone strength analysis using clinical computed tomography scans. *Ann N Y Acad Sci.* 2010;1192:57–65.
  45. Keaveny TM, Donley DW, Hoffmann PF, Mitlak BH, Glass EV, San Martin JA. Effects of teriparatide and alendronate on vertebral strength as assessed by finite element modeling of QCT scans in women with osteoporosis. *J Bone Miner Res.* 2007;22:149–157.
  46. Keaveny TM, Wachtel EF, Ford CM, Hayes WC. Differences between the tensile and compressive strengths of bovine tibial trabecular bone depend on modulus. *J Biomech.* 1994;27:1137–1146.
  47. Kuhn JL, Goldstein SA, Choi K, London M, Feldkamp LA, Matthews LS. Comparison of the trabecular and cortical tissue moduli from human iliac crests. *J Orthop Res.* 1989;7:876–884.
  48. Kuhn LT, Grynpas MD, Rey CC, Wu Y, Ackerman JL, Glimcher MJ. A comparison of the physical and chemical differences between cancellous and cortical bovine bone mineral at two ages. *Calcif Tissue Int.* 2008;83:146–154.
  49. Lambert JB, Simpson SV, Buikstra JE, Hanson D. Electron microprobe analysis of elemental distribution in excavated human femurs. *Am J Phys Anthropol.* 1983;62:409–423.
  50. Lane NE, Yao W, Balooch M, Nalla RK, Balooch G, Habelitz S, Kinney JH, Bonewald LF. Glucocorticoid-treated mice have localized changes in trabecular bone material properties and osteocyte lacunar size that are not observed in placebo-treated or estrogen-deficient mice. *J Bone Miner Res.* 2006;21:466–476.
  51. Lang TF, Leblanc AD, Evans HJ, Lu Y. Adaptation of the proximal femur to skeletal reloading after long-duration spaceflight. *J Bone Miner Res.* 2006;21:1224–1230.
  52. Link TM. Correlations between joint morphology and pain and between magnetic resonance imaging, histology, and micro-computed tomography. *J Bone Joint Surg Am.* 2009;91(Suppl 1):30–32.
  53. Link TM, Majumdar S. Current diagnostic techniques in the evaluation of bone architecture. *Curr Osteoporos Rep.* 2004;2:47–52.
  54. Liu-Ambrose TY, Khan KM, Eng JJ, Heinonen A, McKay HA. Both resistance and agility training increase cortical bone density in 75- to 85-year-old women with low bone mass: a 6-month randomized controlled trial. *J Clin Densitom.* 2004;7:390–398.
  55. MacNeil JA, Boyd SK. Accuracy of high-resolution peripheral quantitative computed tomography for measurement of bone quality. *Med Eng Phys.* 2007;29:1096–1105.
  56. Majumdar S, Genant HK, Grampp S, Newitt DC, Truong VH, Lin JC, Mathur A. Correlation of trabecular bone structure with age, bone mineral density, and osteoporotic status: in vivo studies of the distal radius using high resolution magnetic resonance imaging. *J Bone Miner Res.* 1997;12:111–118.
  57. Majumdar S, Kothari M, Augat P, Newitt DC, Link TM, Lin JC, Lang T, Lu Y, Genant HK. High-resolution magnetic resonance imaging: three-dimensional trabecular bone architecture and biomechanical properties. *Bone.* 1998;22:445–454.
  58. Marshall D, Johnell O, Wedel H. Meta-analysis of how well measures of bone mineral density predict occurrence of osteoporotic fractures. *BMJ.* 1996;312:1254–1259.
  59. Moore JR, Garrido L, Ackerman JL. Solid state phosphorus-31 magnetic resonance imaging of bone mineral. *Magn Reson Med.* 1995;33:293–299.
  60. Morgan EF, Keaveny TM. Dependence of yield strain of human trabecular bone on anatomic site. *J Biomech.* 2001;34:569–577.
  61. Morgan EF, Mason ZD, Chien KB, Pfeiffer AJ, Barnes GL, Einhorn TA, Gerstenfeld LC. Micro-computed tomography assessment of fracture healing: relationships among callus structure, composition, and mechanical function. *Bone.* 2009;44:335–344.
  62. Muller R, van Lenthe GH. Trabecular bone failure at the microstructural level. *Curr Osteoporos Rep.* 2006;4:80–86.
  63. Nyman JS, Ni Q, Nicolella DP, Wang X. Measurements of mobile and bound water by nuclear magnetic resonance correlate with mechanical properties of bone. *Bone.* 2008;42:193–199.
  64. Oliver WC, Pharr GM. Improved technique for determining hardness and elastic modulus using load and displacement sensing indentation experiments. *J Mater Res.* 1992;7:1564–1583.
  65. Parfitt AM, Drezner MK, Glorieux FH, Kanis JA, Malluche H, Meunier PJ, Ott SM, Recker RR. Bone histomorphometry: standardization of nomenclature, symbols, and units: report of the ASBMR Histomorphometry Nomenclature Committee. *J Bone Miner Res.* 1987;2:595–610.
  66. Peyrin F, Salome M, Cloetens P, Laval-Jeantet AM, Ritman E, Ruegsegger P. Micro-CT examinations of trabecular bone samples at different resolutions: 14, 7 and 2 micron level. *Technol Health Care.* 1998;6:391–401.
  67. Pistoia W, van Rietbergen B, Laib A, Ruegsegger P. High-resolution three-dimensional-pQCT images can be an adequate basis for in-vivo microFE analysis of bone. *J Biomech Eng.* 2001;123:176–183.
  68. Reilly DT, Burstein AH. The elastic and ultimate properties of compact bone tissue. *J Biomech.* 1975;8:393–405.
  69. Rho JY, Roy ME 2nd, Tsui TY, Pharr GM. Elastic properties of microstructural components of human bone tissue as measured by nanoindentation. *J Biomed Mater Res.* 1999;45:48–54.
  70. Roschger P, Fratzl-Zelman N, Misof BM, Glorieux FH, Klaushofer K, Rauch F. Evidence that abnormal high bone mineralization in growing children with osteogenesis imperfecta is not associated with specific collagen mutations. *Calcif Tissue Int.* 2008;82:263–270.

71. Roschger P, Manjubala I, Zoeger N, Meirer F, Simon R, Li C, Fratzl-Zelman N, Misof B, Paschalis E, Streli C, Fratzl P, Klaushofer K. Bone material quality in transiliac bone biopsies of postmenopausal osteoporotic women after 3 years of strontium ranelate treatment. *J Bone Miner Res.* 2010;25:891–900.
72. Roschger P, Paschalis EP, Fratzl P, Klaushofer K. Bone mineralization density distribution in health and disease. *Bone.* 2008;42:456–466.
73. Ruegsegger P, Koller B, Muller R. A microtomographic system for the nondestructive evaluation of bone architecture. *Calcif Tissue Int.* 1996;58:24–29.
74. Schulmerich MV, Cole JH, Kreider JM, Esmonde-White F, Dooley KA, Goldstein SA, Morris MD. Transcutaneous Raman spectroscopy of murine bone in vivo. *Appl Spectrosc.* 2009;63:286–295.
75. Sell DR, Monnier VM. Isolation, purification and partial characterization of novel fluorophores from aging human insoluble collagen-rich tissue. *Connect Tissue Res.* 1989;19:77–92.
76. Tang SY, Zeenath U, Vashishth D. Effects of non-enzymatic glycation on cancellous bone fragility. *Bone.* 2007;40:1144–1151.
77. Techawiboonwong A, Song HK, Leonard MB, Wehrli FW. Cortical bone water: in vivo quantification with ultrashort echo-time MR imaging. *Radiology.* 2008;248:824–833.
78. Tseng KF, Bonadio JF, Stewart TA, Baker AR, Goldstein SA. Local expression of human growth hormone in bone results in impaired mechanical integrity in the skeletal tissue of transgenic mice. *J Orthop Res.* 1996;14:598–604.
79. Turner CH, Burr DB. Basic biomechanical measurements of bone: a tutorial. *Bone.* 1993;14:595–608.
80. van der Meulen MC, Jepsen KJ, Mikic B. Understanding bone strength: size isn't everything. *Bone.* 2001;29:101–104.
81. Vashishth D. The role of the collagen matrix in skeletal fragility. *Curr Osteoporos Rep.* 2007;5:62–66.
82. Voide R, Schneider P, Stauber M, Wyss P, Stampanoni M, Sennhauser U, van Lenthe GH, Muller R. Time-lapsed assessment of microcrack initiation and propagation in murine cortical bone at submicrometer resolution. *Bone.* 2009;45:164–173.
83. Waarsing JH, Day JS, van der Linden JC, Ederveen AG, Spanjers C, De Clerck N, Sasov A, Verhaar JA, Weinans H. Detecting and tracking local changes in the tibiae of individual rats: a novel method to analyse longitudinal in vivo micro-CT data. *Bone.* 2004;34:163–169.
84. Wehrli FW, Fernandez-Seara MA. Nuclear magnetic resonance studies of bone water. *Ann Biomed Eng.* 2005;33:79–86.
85. Wu Y, Ackerman JL, Chesler DA, Li J, Neer RM, Wang J, Glimcher MJ. Evaluation of bone mineral density using three-dimensional solid state phosphorus-31 NMR projection imaging. *Calcif Tissue Int.* 1998;62:512–518.
86. Wu Y, Chesler DA, Glimcher MJ, Garrido L, Wang J, Jiang HJ, Ackerman JL. Multinuclear solid-state three-dimensional MRI of bone and synthetic calcium phosphates. *Proc Natl Acad Sci USA.* 1999;96:1574–1578.
87. Wu Y, Hrovat MI, Ackerman JL, Reese TG, Cao H, Ecklund K, Glimcher MJ. Bone matrix imaged in vivo by water- and fat-suppressed proton projection MRI (WASPI) of animal and human subjects. *J Magn Reson Imaging.* 2010;31:954–963.
88. Ziv V, Wagner HD, Weiner S. Microstructure-microhardness relations in parallel-fibered and lamellar bone. *Bone.* 1996;18:417–428.
89. Zysset PK. Indentation of bone tissue: a short review. *Osteoporos Int.* 2009;20:1049–1055.